Alfaro, Laura; Faia, Ester; Lamersdorf, Nora; Saidi, Farzad

Working Paper

Social interactions in a pandemic

ECONtribute Discussion Paper, No. 110

Provided in Cooperation with:
Reinhard Selten Institute (RSI), University of Bonn and University of Cologne

Suggested Citation: Alfaro, Laura; Faia, Ester; Lamersdorf, Nora; Saidi, Farzad (2021) : Social interactions in a pandemic, ECONtribute Discussion Paper, No. 110, University of Bonn and University of Cologne, Reinhard Selten Institute (RSI), Bonn and Cologne

This Version is available at:
https://hdl.handle.net/10419/244344

ECONtribute
MARKETS & PUBLIC POLICY

ECONtribute
Discussion Paper No. 110

Social Interactions in a Pandemic

Laura Alfaro
Ester Faia
Nora Lamersdorf
Farzad Saidi

August 2021

www.econtribute.de

UNIVERSITÄT BONN
Universität zu Köln

Funding by the Deutsche Forschungsgemeinschaft (DFG, German Research Foundation) under Germany´s Excellence Strategy – EXC 2126/1– 390838866 is gratefully acknowledged.

Social Interactions in a Pandemic*

Laura Alfaro†
Harvard Business School and NBER

Ester Faia‡
Goethe University Frankfurt and CEPR

Nora Lamersdorf§
Goethe University Frankfurt

Farzad Saidi¶
University of Bonn and CEPR

August 6, 2021

Abstract

Externalities and social preferences, such as patience and altruism, play a key role in the endogenous choice of social interactions, which in turn affect the diffusion of a pandemic or patterns of social segregation. We build a dynamic model, augmented with an SIR block, in which agents optimally choose the intensity of both general and group-specific social interactions. The equilibria in the baseline and the SIR-network model result from a matching process governed by optimally chosen contact rates. Taking into account agents' endogenous behavior generates markedly different predictions relative to a naïve SIR model. Through a planner's problem, we show that neglecting agents' response to risk leads to misguided policy decisions. Mobility restrictions beyond agents' restraint are needed to the extent that aggregate externalities are not curtailed by social preferences.

Keywords: *social interactions, pandemics, SIR network models, social preferences, social planner, targeted policies.*

JEL Codes: D62, D64, D85, D91, E70, I10, I18.

∗ We thank John Cochrane, Pietro Garibaldi, Maximilian Mayer, Krisztina Molnar, Dirk Niepelt, Vincenzo Pezone and Venky Venkateswaran, as well as seminar participants for their comments and suggestions. Faia gratefully acknowledges funding by the DFG under grant FA-1022-2, and Saidi's research is funded by the Deutsche Forschungsgemeinschaft (DFG, German Research Foundation) under Germany's Excellence Strategy (EXC 2126/1 – 390838866).
† E-mail: lalfaro@hbs.edu
‡ E-mail: faia@wiwi.uni-frankfurt.de
§ E-mail: lamersdorf@econ.uni-frankfurt.de
¶ E-mail: saidi@uni-bonn.de

1. Introduction

The structure of social networks may entail externalities, positive or negative. Furthermore, different societies and cultures exhibit different social preferences.[1] Both affect the choice of agents with respect to the intensity of their social interactions. However, these phenomena are often studied with exogenous network models that neglect agents' behavioral decisions. Taking into account how social interactions change in response to incentives, costs, and externalities is crucial to correctly assess the dynamics of social networks. The latter, in turn, are crucial determinants of a variety of phenomena that range from the diffusion of pandemics to the shape of social segregation. The goal of this paper is to provide a model in which agents optimally choose contact probabilities, based on their social preferences, which govern the structure of social networks through a matching process.

Specifically, we build a decision-theoretical model in which agents choose social interactions so as to maximize their lifetime utility and internalize costs and externalities of social contacts. We allow for the inclusion of social preferences, such as altruism, so agents can internalize the consequences of their interactions on others. Given the optimally chosen contact probabilities, the equilibrium is then achieved through a search and matching process. Ultimately, individual preferences (patience), social preferences (altruism), and the technological properties of the matching function, which captures the degree of geographical congestion, jointly affect the equilibrium solution of the social network. Finally, through a social planner's problem we devise optimal policies in this framework by taking into account all the externalities of agents' optimally chosen interactions.

While this model can have several applications (e.g., information-diffusion networks, or networks with endogenous homophily and segregation), we apply it to the recent COVID-19 pandemic. There has been an increasing understanding that the traditional epidemiological models are ill-equipped to make predictions due to the lack of agents' behavioral response. The standard SIR model[2] (either with homogeneous contacts or with a network structure),

1 See, for instance, Falk et al. (2018), Hofstede (2001), or Spolaore and Wacziarg (2013) among others.

2 SIR stands for "S," the number of susceptible, "I," the number of infectious, and "R," the number of recovered, deceased, or immune individuals.

which has been the main toolkit for predicting the spread of viral diseases since 1927, assumes that contacts among agents are exogenous. However, human beings react to risk and to policy decisions, and adapt their behavior accordingly. If these decisions are made in neglect of behavioral reactions, they are most likely misguided.

Our specific model application to the pandemic features an SIR block, in which the probability of becoming infected is endogenous. Susceptible individuals internalize the future risk of infection and its costs, conditionally on their degree of patience. Infected individuals internalize the infection risk only to the extent that they hold altruistic preferences. The endogenous choice of social activity affects the probability of getting in contact with others, and thus the matching process, which finally governs the infection probability.

We highlight the role of aggregate externalities (risk of infection), individual traits (patience), social preferences[3] (altruism), and geographical features (urban congestion as captured by the degree of homogeneity of the matching function) in affecting the optimal choice of social interactions and, in turn, the spread of the disease. In the model, for instance, a susceptible individual internalizes the infection risk more when being more patient. We also consider a network variant of the model where different groups have varying contact rates, depending on their degrees of homophily, and different recovery rates from the disease. When a community is hit by COVID-19, age groups are differentially exposed to health risk and, depending on the structure of the community, their interaction might be more or less intense. In a model with dynamic choice of social interactions, the degree of homophily gives rise to differential reciprocal relations, as, e.g., agents internalize more the future risk of infections of those with whom they interact more frequently. So far, even more modern variants of this class of models, which account for the heterogeneous topology of contact networks, still assume exogenous contact rates – something that is starkly at odds with the decision process characterizing human behavior.

Our numerical simulations show that the predictions of our model, in all of its variants, deviate sharply from those of the naïve SIR model with exogenous contact rates, with or without a network structure. In particular, simulations of model variants where agents adjust

3 See Berg et al. (1995), Bohnet and Frey (1999), Andreoni (1989), and Andreoni (1993).

their social activity in response to risk, altruism, and homophily all exhibit a significantly flattened infection curve compared to the traditional SIR model. Altruism also implies that susceptible individuals have to reduce their social interactions by less, as part of the burden of flattening the curve is borne by the infected individuals. A lower degree of homophily in the SIR-network model implies that, for example, younger agents meet older agents more frequently, so they internalize their risk by more. If they are altruistic, they take into account the lower recovery rates of the older agents and adjust their behavior accordingly. However, old susceptible individuals reduce their social activity relatively more due to their higher health risk.

Equipped with this model of human behavior, we study the design of optimal policy and its implementation through various non-pharmaceutical interventions (henceforth NPIs). In contrast to policy decisions derived from the naïve SIR model, a social planner may still want to restrict interactions beyond agents' endogenous restraints. This is, however, due to the emergence of aggregate externalities. We specifically point out the role of a static-congestion and a dynamic-commitment inefficiency of the decentralized outcome. The planner internalizes the effect of individual social activities on the overall congestion of a community, which leads to a static inefficiency. The planner is also aware that her policies can affect the future number of infected individuals, which in turn gives rise to a dynamic inefficiency.[4] We decompose the two inefficiencies, and show that they depend, among others, on the matching technology's returns to scale, which capture location density and infrastructure. In the SIR-network model, an additional inefficiency arises since the planner also internalizes the differential impact that the activity of each group has on the average infection rate of the others based on their degrees of differential attachment and, thus, contact rates.

Analytically, we show that lockdown policies targeted toward certain groups are implementable only when identification of infected individuals is possible. Simulations allow us to quantify the optimal lockdown policies. We find that the optimal share of locked-down activities is smaller in the presence of altruism. In the SIR-network model, a social planner chooses stricter stringency measures for agents with higher infection probability (possibly the

4 This is similar to Moser and Yared (2020), in that we highlight a dynamic inefficiency compared to the social planner's commitment.

younger ones) and when groups exhibit less differential attachment, as in that case the disease is less likely to be confined to one group, and can spread more easily within communities.

It is important to note that while we devise our framework with a specific application in mind, namely the pandemic, the validity of our model extends beyond and can be used to study other social phenomena, such as information diffusion or social and racial segregation. For instance, in a model of information diffusion, the utility cost of contact represents the time cost of acquiring information from others, and the future spillovers could represent either positive information externalities or the risk of competing rents from innovations. Similarly, our model can be used to study endogenous homophily, with the utility cost representing again the time cost of investing in relationships and the future spillovers representing costs and benefits of reciprocity.

Relation to Literature. There is important evidence on the role and interaction between beliefs, individuals' optimizing decisions, and social networks (see Bailey et al. (2018)), also during the pandemic (see Bailey et al. (2020)). Yet, the theoretical literature is lacking corresponding advances on the front of endogenous (social) networks.

While we devise an application to the pandemic, our theory belongs and contributes to the class of models used to study endogenous social-network formation within a search-theoretic context. Work on social capital goes back to Becker (1996). Endogenous social interactions were first formalized in an equilibrium model by Brock and Durlauf (2001). The impact of social interactions on neighborhoods or social structures are covered by Case and Katz (1991) and Glaeser et al. (1996). Closest to our model is that by Currarini et al. (2009), who study the formation of links through utility maximization and the emergence of homophily through a biased search and matching process. Their goal is to explain patterns of segregation and homophily in societies. Much like them, we study endogenous social interactions also in a network context with utility-maximizing agents and a search and matching process. Our model differs from theirs in that our agents solve dynamic-optimization problems, and we analyze both a decentralized equilibrium as well as the social planner's problem. The idea of differential homophily is also in line with the social-interaction comparative advantage

proposed in Cicala et al. (2018). More recently, Wu and Shimer (2021) also study networks with endogenous homophily in which agents atomistically choose the contact probability.

Our paper also relates to the literature on informal insurance in random and social networks. This literature studies how transfers and obligations translate into global risk sharing (see Ambrus et al. (2014), Bloch et al. (2008), or Bramoullé and Kranton (2007)). As in these models, links, whether random or directed, have utility values, and social interactions are chosen by sharing the infection risk within a community.

The literature on the economics of pandemics is vast. Any feasible list would be incomplete at this point, hence we focus on the papers closely and strictly related to ours. One notion that is rapidly gaining ground relates to the fact that any model, no matter how encompassing in terms of agents, geographical locations, and economic sectors,[5] might have low predictive power, identification problems, and might lead to naïve policy prescriptions if it neglects the role of agents' reaction and, most importantly in this context, the role of social preferences. Papers that have addressed this issue independently, also in a search-theoretic context, are Garibaldi et al. (2020) and Farboodi et al. (2020). Note that the search-theoretic context is crucial in addressing the coordination externalities in public health domains. These papers, however, do not examine the network component, the role of social preferences, and their interaction with the coordination externalities. Acemoglu et al. (2020) present an SIR-network with multiple age groups. Contacts are exogenous. Recently, Wu and Shimer (2021) have applied an endogenous network model to the pandemic.

2. Limitations of SIR and SIR-Network Models

Before turning to our model with optimizing social contacts, it is useful to motivate our study and mostly our application to the pandemic by reviewing the traditional model used for epidemics diffusion. That model can be used more generally to study diffusion, also within

5 In fact, there is already a large literature in epidemiology that studies SIR-network models with bosonic-type reaction-diffusion processes (see, for instance, Pastor-Satorras and Vespignani (2001a,b)) or activity-driven SIR-network models (Moinet et al. (2018) and Perra et al. (2012)).

networked societies. However its main drawback is the exogeneity of the contact probabilities, something which weakens its predictions abilities as well as limits its use for policy analysis.

In the basic homogeneous SIR model (see Kermack and McKendrick (1927) or Hethcote (2000) more recently), there are three groups of agents: susceptible (S), infected (I), and recovered (R) ones. The number of susceptible decreases as they are infected. At the same time, the number of infected increases by the same amount, but also declines because people recover. Recovered people are immune to the disease and, hence, stay recovered. The mathematical representation of the model is as follows:

$$S_{t+1} = S_t - \lambda_t I_t S_t \tag{1}$$

$$I_{t+1} = I_t + \lambda_t I_t S_t - \gamma I_t \tag{2}$$

$$R_{t+1} = R_t + \gamma I_t, \tag{3}$$

where $N = S_t + I_t + R_t$ is the overall population and λ_t is the transmission rate of the infection.

Hence, $p_t = \lambda_t I_t$ is the probability that a susceptible individual becomes infected at time t. In the classic model, the latter is assumed to be exogenous, constant, and homogeneous across groups. Even as agents become aware of the pandemic, it is assumed that they do not adjust their behavior. More recent versions of the SIR model incorporate the dependence of contact rates on the heterogeneous topology of the network of contacts and mobility of people across locations (see Pastor-Satorras and Vespignani (2001a,b) who include bosonic-type reaction-diffusion processes in SIR models). Other variants of the model incorporate the dependence of infection rates on the activity intensity of each node of the network (see Perra et al. (2012) for solving activity-driven SIR using mean-field theory and Moinet et al. (2018) who also introduce a parameter capturing an exogenous decay of the infection risk due to precautionary behavior).

In what follows, we develop a model of endogenous social interactions, augmented with either a homogeneous SIR and or a SIR-network block to show how behavioural response can change affect interactions and diffusion of disease during a pandemic.

3. A Model of Decision Theory-Based Social Interactions for Pandemics

We develop a model in which the contact rate results from a decision problem on the extent of social interactions. Combining search and optimizing behavior in economics goes back to Diamond (1982).[6] We insert this optimizing search and matching structure within a SIR structure, with three group of agents (susceptible, infected and recovered) facing different incentives and costs for interactions. Susceptible agents internalize the probability of getting infected, which also entail a utility cost. The dynamic optimization allows us to control also for time discounting or patience. More patient individuals assign a higher weight to future risk of infection. Furthermore, we consider the model in two variants: one with a single group of individuals (which can be in either of the SIR states) and a networked structure with multiple groups. In this second variant we will assume that agents have different costs of contacting each other (the risk of infection and recovery in the specific epidemic application) and that have different contact rates (either exogenously or endogenously chosen).

A key distinguishing feature of our model is the inclusion of social preferences that also affect the choice of social interaction, and in turn of the spread of the disease. Infected agents internalize the health risk for others only under altruistic preferences.[7] In the model, warm-glow preferences are used to capture aspects common to altruism or trust.

Importantly social externalities emerge in our model, as each individual behaviour affects the risk of infection of others. It is this and other dynamic externalities that call for the a planner intervention. We stress that a planner problem that neglects the behavioural response of individuals would lead to misguided conclusions.

At last as mentioned earlier our model is amenable to other applications. In an information diffusion model the utility cost of a contact would capture the time-cost of acquiring information from others and future utility of becoming informed may entail information

6 See Petrongolo and Pissarides (2001) for a survey.

7 Such setup implicitly assumes that agents recognize their symptoms. As known, there are also asymptomatic agents. Extending our model so as to incorporate the latter would not affect the main channels that we discuss.

spillovers. Similarly the model could be used to model endogenous homphily and friendship, where again the utility cost of the contact represent the time and effort costs of maintaining relations.

3.1. Dynamic Optimization

For exposition reasons we start with the homogeneous case where all agents in the population are the same except that they are susceptible, infected, or recovered. We label the health status with the index $i \in \{S, I, R\}$. Transitions of susceptible individuals from state S to I depend on contacts with other people,[8] and these in turn depend on the social-activity intensity of each individual in the population and on the general matching technology.[9] The model is in discrete time, time goes up to the infinite horizon, and there is no aggregate or idiosyncratic uncertainty.

Each agent has a per-period utility function $U_t^i(x_{h,t}^i, x_{s,t}^i) = u^i(x_{h,t}^i, x_{s,t}^i) - c^i(x_{h,t}^i, x_{s,t}^i)$, where x_h^i denotes home activities and x_s^i denotes social activities. The function $u^i(x_h^i, x_s^i)$ has standard concavity properties and $u^i(x_h^i, 0) > 0$. The cost, $c^i(x_h^i, x_s^i)$, puts a constraint on the choice between home and social activities. At time t, a susceptible agent enjoys the per-period utility, expects to enter the infected state with probability p_t or to remain susceptible with probability $(1 - p_t)$, and chooses the amount of home and social activities by recognizing that social activity increases the risk of infection. The value function of a susceptible individual is as follows:

$$V_t^S = U(x_{h,t}^S, x_{s,t}^S) + \beta[p_t V_{t+1}^I + (1 - p_t)V_{t+1}^S], \tag{4}$$

where β is the time discount factor, corresponding to $Patience_g$ in the data, while p_t is the probability of being infected. The latter depends on the amount of social activity of the susceptible and infected agents, on the average amount of social activity, $\bar{x}_{s,t}$, in the

8 These can arise in, e.g., entertainment activities, other outside activities, or in the workplace.

9 Transitions for individuals in the infected group I to recovery R depend only on medical conditions related to the disease (mostly the health system) that are outside of an individual's control.

population, an exogenously given transmission rate η, capturing the transmissibility of the disease, as well as on the individual shares of each group $i = I, S, R$ in the population:

$$p_t = p_t(x^S_{s,t}, x^I_{s,t}, \bar{x}_{s,t}, \eta, S_t, I_t, R_t), \tag{5}$$

where

$$\bar{x}_{s,t} = \bar{x}^S_{s,t}\frac{S_t}{N_t} + \bar{x}^I_{s,t}\frac{I_t}{N_t} + \bar{x}^R_{s,t}\frac{R_t}{N_t} \tag{6}$$

and $\bar{x}^S_{s,t}$ is the average amount of social activity of the susceptible, $\bar{x}^I_{s,t}$ is the average amount of social activity of the infected and $\bar{x}^R_{s,t}$ is the average amount of social activity of the recovered.

To map the endogenous SIR model to the standard SIR model in equations (1) to (3), the following convention is used: $p_t = \lambda_t I_t$. The exact functional form of p_t is defined later on. For now, it suffices to assume that $\frac{\partial p_t(.)}{\partial x^S_{s,t}} > 0$ and $p_t(0, .) = 0$.

In the baseline model, infected individuals do not have any altruistic motive. This specification allows us to highlight clearly the role of altruism once introduced. Their Bellman equation, in absence of altruism, is:

$$V^I_t = U(x^I_{h,t}, x^I_{s,t}) + \beta[(1-\gamma)V^I_{t+1} + \gamma V^R_{t+1}]. \tag{7}$$

Currently infected individuals will remain infected for an additional period with probability $(1-\gamma)$ or will recover with probability γ.[10] The value function of the recovered reads as follows:

$$V^R_t = U(x^R_{h,t}, x^R_{s,t}) + \beta V^R_{t+1}. \tag{8}$$

Susceptible individuals' first-order conditions with respect to $x_{h,t}$ and $x_{s,t}$ are as follows:

$$\frac{\partial U(x^S_{h,t}, x^S_{s,t})}{\partial x^S_{h,t}} = 0 \tag{9}$$

$$\frac{\partial U(x^S_{h,t}, x^S_{s,t})}{\partial x^S_{s,t}} + \beta\frac{\partial p_t(.)}{\partial x^S_{s,t}}(V^I_{t+1} - V^S_{t+1}) = 0, \tag{10}$$

10 Infected individuals might have a lower utility than susceptible or recovered ones due to the disease. We capture this in our calibration of the simulated model by assigning an extra cost of being sick in the utility function.

where it is reasonable to assume that $(V^I_{t+1} - V^S_{t+1}) < 0$.

Susceptible individuals internalize the drop in utility associated with the risk of infection caused by social activity, and choose a level of social activity which is lower than the one that they would choose in the absence of a pandemic. This parallels the empirical findings from a companion paper of ours based on Alfaro et al. (2020) insofar as agents naturally reduce their mobility in response to increased fear of infection. Also, individuals reduce social interactions by more when the discount factor, i.e., β, is higher. This mirrors again the empirical results from our companion paper based on Alfaro et al. (2020), namely that the degree of patience reduces mobility and, thus, renders lockdown policies less effective or less necessary.

The first-order conditions of the infected with respect to $x_{h,t}$ and $x_{s,t}$ read as follows:

$$\frac{\partial U(x^I_{h,t}, x^I_{s,t})}{\partial x^I_{h,t}} = 0, \frac{\partial U(x^I_{h,t}, x^I_{s,t})}{\partial x^I_{s,t}} = 0. \tag{11}$$

Infected individuals choose a higher level of social activity than susceptible ones since they do not internalize the effect of their decision on the risk of infection for others. However, their level of social activity will in turn affect the overall infection rate. In Section 3.3, we will assume infected individuals to hold altruistic preferences. This will induce them to also internalize the effect of their actions on the infection rate of the susceptible.

Finally, the first-order conditions of the recovered individuals are as follows:

$$\frac{\partial U(x^R_{h,t}, x^R_{s,t})}{\partial x^R_{h,t}} = 0, \frac{\partial U(x^R_{h,t}, x^R_{s,t})}{\partial x^R_{s,t}} = 0. \tag{12}$$

Recovered people, assuming that they are immune to another infection, choose the same level of social activity as they would in the absence of a pandemic.

3.2. The Matching Function, Geography, and the Infection Rate

Given the optimal choice of social-activity intensity, we can now derive the equilibrium infection probability in the decentralized equilibrium. This involves defining a matching function (similar to the ones in Diamond (1982) or Pissarides (2000)). The intensity of social

interaction, x_s, corresponds to the number of times people leave their home or, differently speaking, the probability per unit of time of leaving the home. In each one of these outside activities, individuals come in contact with other individuals. How many contacts the susceptible individuals have with an infected individual depends on the average amount of social activities in the population. Given (6) and normalizing the population size to one, the latter is given by $\bar{x}_{s,t} = S_t\bar{x}^S_{s,t} + I_t\bar{x}^I_{s,t} + R_t\bar{x}^R_{s,t}$. More precisely, the aggregate number of contacts depends on a matching function, which itself depends on the aggregate average social activity, $\bar{x}_{s,t}$, and can be specified as follows: $m(\bar{x}^S_{s,t}, \bar{x}^I_{s,t}, \bar{x}^I_{s,t}) = (\bar{x}_{s,t})^\alpha$.

The parameter α captures the matching function's returns to scale, ranging from constant to increasing. As such, this parameter captures, e.g., the geographic aspects of the location in which the disease spreads. Cities with denser logistical structures induce a larger number of overall contacts per outside activity. These could be, for example, cities with highly ramified underground transportation systems. In such locations, citizens tend to use public transport more frequently, and their likelihood of encountering infected individuals is subsequently larger. Mapping the geographical diversity is important also since our empirical analysis suggests that the uptake of public transit reacts more to fear (see our empirical evidence in Alfaro et al. (2020)).

Given the aggregate number of contacts, the average number of contacts per outside activity is given by $\frac{m(\bar{x}_{s,t})}{\bar{x}_{s,t}}$. Under the matching-function specification adopted above, this can be written as $(\bar{x}_{s,t})^{(\alpha-1)}$. The probability of becoming infected depends also on the joint probability that susceptible and infected individuals both go out, which is given by $x^s_{s,t}x^I_{s,t}$, on the infection transmission rate, η, and on the number of infected individuals in the population, I_t. Therefore, we can denote the infection probability in the decentralized equilibrium as:

$$p_t(.) = \eta x^S_{s,t}x^I_{s,t}\frac{m(\bar{x}^S_{s,t}, \bar{x}^I_{s,t}, \bar{x}^R_{s,t})}{\bar{x}_{s,t}}I_t = \eta x^S_{s,t}x^I_{s,t}(\bar{x}_{s,t})^{\alpha-1}I_t. \tag{13}$$

Note that atomistic agents take the fraction of outside activities of other agents as given. If $\alpha = 0$, the probability $p_t = \eta x^S_{s,t}x^I_{s,t}\bar{x}^{-1}_{s,t}I_t$ is homogeneous of degree one, implying constant

returns to scale, while if $\alpha = 1$, the probability becomes a quadratic function (see Diamond (1982)), as a consequence of which it exhibits increasing returns to scale.

The baseline SIR model in the decentralized equilibrium can now be re-written as follows:

$$S_{t+1} = S_t - p_t S_t \tag{14}$$

$$I_{t+1} = I_t + p_t S_t - \gamma I_t \tag{15}$$

$$R_{t+1} = R_t + \gamma I_t, \tag{16}$$

where $S_t + I_t + R_t \equiv 1$.

Definition 1. *A decentralized equilibrium is a sequence of state variables, S_t, I_t, R_t, a set of value functions, V_t^S, V_t^I, V_t^R, and a sequence of home consumption, probabilities, and social activities, $p_t, x_{h,t}^S, x_{h,t}^I, x_{h,t}^R, x_{s,t}^S, x_{s,t}^I, x_{s,t}^R$, such that:*

1. S_t, I_t, R_t solve (14) to (16), with the probability of infection given by (13)
2. V_t^S, V_t^I, V_t^R solve (4), (7), and (8)
3. The sequence $p_t, x_{h,t}^S, x_{h,t}^I, x_{h,t}^R, x_{s,t}^S, x_{s,t}^I, x_{s,t}^R$ solves (9), (10), (11), and (12).

Note that underlying the decentralized economy is a Nash symmetric equilibrium in the choice of social intensity.[11]

3.3. Altruism of Infected Individuals

Our empirical results have highlighted that the degrees of altruism and trust matter. Those two traits include variants of more or less selfish thinking. Altruism might arise from the pure pleasure of doing good, while trust embeds some degree of future reciprocation and is more generalized towards strangers.[12] In the model, we aim to mimic these traits. Specifically, warm-glow preferences are used to capture common features of altruism and trust, namely the utility enhancement of doing good. It is reasonable to conjecture that infected individuals hold some altruistic preferences. These attitudes may include both warm-glow preferences

11 Ultimately, this can be micro-founded with global-games and higher-thinking considerations.
12 See Berg et al. (1995), Bohnet and Frey (1999), Andreoni (1989), or Andreoni (1993).

towards relatives and friends (see Becker (1974))[13] or general unconditional altruism and social preferences.[14] For this reason, we now extend the per-period utility so as to incorporate altruistic preferences by defining it as follows:

$$U(x^I_{h,t}, x^I_{s,t}) = u(x^I_{h,t}, x^I_{s,t}) - c(x^I_{h,t}, x^I_{s,t}) + \delta V^S_t. \tag{17}$$

While infected individuals do not internalize the effect of their social activities on the infection rate fully, as they are already immune in the near future, they do hold an altruistic motive towards the susceptible, which is captured by a weight $\delta \in (0, 1)$. The first-order condition with respect to the social activity changes to:

$$\frac{\partial U(x^I_{h,t}, x^I_{s,t})}{\partial x^I_{s,t}} + \delta\beta \frac{\partial p_t(.)}{\partial x^I_{s,t}}(V^I_{t+1} - V^S_{t+1}) = 0. \tag{18}$$

Now the optimal level of social activity chosen by infected individuals is lower than the one obtained under (11) since they partly internalize the risk of infecting susceptible individuals, who then turn into infected ones next period. Time discounting is also relevant in this context: more patient individuals tend to internalize the impact of their social activity on the infection probability by more.

3.4. Extension to an SIR-Network Model

Within communities there are different groups that have different exposure or contact rates to each one of the other groups. The intensity of these contacts across groups can be characterized by the degree of homophily. It describes "the tendency of various types of individuals to associate with others who are similar to themselves" (Currarini et al. (2009)).[15] In networks, a high degree of homophily implies that two nodes (groups) are linked only to a small degree to each other. Currarini et al. (2009) show that social networks exhibit typically both high homophily and reciprocity. In our context with dynamic decisions on

13 Warm-glow preferences have a long-standing tradition in economics. Besides Becker (1974)'s original work, see Andreoni (1989) as well as Andreoni (1993).

14 See, for instance, Bolton and Ockenfels (2000) or Andreoni and Miller (2002).

15 See also Fehr and Schmidt (1999) or Fehr and Gächter (2000).

social interactions and externalities, the degree of homophily can be linked to the extent of reciprocity towards individuals of one's own and of other groups. If two groups have lower homophily, and, hence, have more frequent contacts with other groups, they will internalize their relative risk of infection. We extend the SIR model so as to include different groups of the population that experience different contact rates due to differential degrees of homophily. These groups could correspond to, e.g., the age structure, different strengths in ties, or closer face-to-face interactions in the workplace. The underlying idea is that contact rates tend to be higher among peer groups.

Consider a population with different groups $j = 1, ..., J$. The number of people in each group is N_j. Groups have different probabilities of encounters with the other groups. The contact intensity between group j and any group k is $\xi_{j,k}$. The latter captures differential degrees of attachment within groups. Younger individuals tend to meet other young ones, i.e., their peers, more often. Also, workers in face-to-face occupations enter more often in contacts with workers performing similar tasks. This implies that the infection outbreak may be concentrated among members of the same group. Whether the outbreak then spreads to the rest of the network, and how fast it does so, depends on the relative degree of attachment of the initially infected group to the other groups. At last, in our simulations we realistically allow for differential recovery rates in different age groups, with older agents being more fragile than younger ones.

Each susceptible individual of group j experiences a certain number of contacts per outing with infected individuals of his own group, but also of the other groups. Reflecting our discussion in Section 3.2, the number of contacts experienced by group j depends on the average level of social activity in each group k weighted by the contact intensity across groups, and is equal to:

$$m^j(\hat{x}^j_{s,t}) = m^j\left(\sum_k \xi_{j,k}(\bar{x}^{S,k}_{s,t} S^k_t + \bar{x}^{I,k}_{s,t} I^k_t + \bar{x}^{R,k}_{s,t} R^k_t)\right). \tag{19}$$

As before, the matching function can be specified as $m^j(\hat{x}^j_{s,t}) = \left(\sum_k \xi_{j,k}(\bar{x}^{S,k}_{s,t} S^k_t + \bar{x}^{I,k}_{s,t} I^k_t + \bar{x}^{R,k}_{s,t} R^k_t)\right)^{\alpha}$. The probability of infection of a susceptible person in group j is modified as follows:

$$p^j_t(.) = x^{S,j}_{s,t} \left[\sum_k \eta \xi_{j,k} x^{I,k}_{s,t} \frac{m^j(\hat{x}^j_{s,t})}{\hat{x}^j_{s,t}} I^k_t \right], \tag{20}$$

where $k = 1, .., J$ and $\xi_{j,j} = 1$. The underlying rationale is equivalent to the one described in the single-group case, except that now the probability of meeting an infected person from any other group k is weighted by the likelihood of the contacts across groups, $\xi_{j,k}$.

The SIR model for each group j then reads as follows:

$$S^j_{t+1} = S^j_t - p^j_t(.) S^j_t \tag{21}$$

$$I^j_{t+1} = I^j_t + p^j_t(.) S^j_t - \gamma^j I^j_t \tag{22}$$

$$R^j_{t+1} = R^j_t + \gamma^j I^j_t, \tag{23}$$

where $\sum_j (S^j_t + I^j_t + R^j_t) \equiv 1$ and γ^j are the group-specific probabilities to recover.

As before, atomistic individuals take the average social activity and the average social encounters as given. The first-order condition for social activity of susceptible individuals belonging to group j now reads as follows:

$$\frac{\partial U(x^{S,j}_{h,t}, x^{S,j}_{s,t})}{\partial x^{S,j}_{s,t}} + \beta \left[\sum_k \eta \xi_{j,k} x^{I,k}_{s,t} \frac{m^j(\hat{x}^j_{s,t})}{\hat{x}^j_{s,t}} I^k_t \right] (V^{I,j}_{t+1} - V^{S,j}_{t+1}) = 0. \tag{24}$$

Each susceptible agent takes the average level of social activity by the others as given. It becomes clear that the differential impact of her social activity on the various groups affects her optimal choice. We can now derive the first-order conditions of the infected. For this purpose, we assume altruistic preferences, which means that infected agents internalize, at least partly, with the weight δ, the impact of their choices on the susceptible agents of all other groups. The first-order condition with respect to social activity is:

$$\frac{\partial U(x^{I,j}_{h,t}, x^{I,j}_{s,t})}{\partial x^{I,j}_{s,t}} + \delta\beta \sum_k x^{S,k}_{s,t} S^k \eta \xi_{k,j} \frac{m^k(\hat{x}^k_{s,t})}{\hat{x}^k_{s,t}} I^j_t (V^{I,k}_{t+1} - V^{S,k}_{t+1}) = 0, \tag{25}$$

where now they internalize the impact of their choices on all three groups, weighted by their respective shares S^k. The first-order conditions for the recovered individuals are the same as in (12), but separately for each group j.

Definition 2. *A decentralized equilibrium for the SIR-network model is a sequence of state variables, S_t^j, I_t^j, R_t^j, a set of value functions, $V_t^{S,j}, V_t^{I,j}, V_t^{R,j}$, and a sequence of home consumption, probabilities, and social activities, $p_t^j, x_{h,t}^{S,j}, x_{h,t}^{I,j}, x_{h,t}^{R,j}, x_{s,t}^{S,j}, x_{s,t}^{I,j}, x_{s,t}^{R,j}$, such that:*

1. S_t^j, I_t^j, R_t^j solve (28) to (30) for each group j, with the probability of infection given by (27) for each group j
2. $V_t^{S,j}, V_t^{I,j}, V_t^{R,j}$ solve (4), (7), and (8), now defined separately for each group j
3. The sequence $p_t^j, x_{h,t}^{S,j}, x_{h,t}^{I,j}, x_{h,t}^{R,j}, x_{s,t}^{S,j}, x_{s,t}^{I,j}, x_{s,t}^{R,j}$ solves (24), (25) , (9), the second part of (11), and (12) for each group j.

3.5. Allowing for Differential Inter-Group Contact Choices

The networked variant of the model considered above allows for the choice of the general degree of social interaction, but assumes that inter-group contact rates are exogenous. This is empirically plausible: the extent to which age peers interact more than cross-age groups is effectively dictated by structural factors, such as the daily family and work routine of individuals, and contains not much of a choice. Our model can, however, be also extended to the case in which individuals choose to differentiate their interactions across groups. Here, we derive such an extension and discuss possible differences with the previous case, which arise mainly in the individual group dynamic, whereas the aggregate dynamic is in fact similar across the two models.

As before, each susceptible individual of group j experiences a certain number of contacts per outing with infected individuals of her own group, but also of the other groups. Contrary

to before, each susceptible agent chooses the average level of social activity with every other group. Hence, the matching function for each group j reads as follows:

$$m^j(\hat{x}^j_{s,t}) = m^j\left(\sum_k(\bar{x}^{S,jk}_{s,t}S^k_t + \bar{x}^{I,jk}_{s,t}I^k_t + \bar{x}^{R,jk}_{s,t}R^k_t)\right), \tag{26}$$

where $\bar{x}^{S,jk}_{s,t}$, $\bar{x}^{I,jk}_{s,t}$, and $\bar{x}^{R,jk}_{s,t}$ are the respective intensities of social activity between each group j and each group k. As before, the matching function can be specified as $m^j(\hat{x}^j_{s,t}) = \left(\sum_k(\bar{x}^{S,jk}_{s,t}S^k_t + \bar{x}^{I,jk}_{s,t}I^k_t + \bar{x}^{R,jk}_{s,t}R^k_t)\right)^\alpha$. The probability of infection of a susceptible person in group j, who gets in contact with infected individuals in all groups k, is modified as follows:

$$p^j_t(.) = \left[\sum_k \eta x^{S,jk}_{s,t}x^{I,kj}_{s,t}\frac{m^j(\hat{x}^{jk}_{s,t})}{\hat{x}^{jk}_{s,t}}I^k_t\right], \tag{27}$$

where $m^j(\hat{x}^{jk}_{s,t})$ defines the contacts between persons from group j and group k, with $k = 1, .., J$.

The SIR model for each group j then reads as follows:

$$S^j_{t+1} = S^j_t - p^j_t(.)S^j_t \tag{28}$$

$$I^j_{t+1} = I^j_t + p^j_t(.)S^j_t - \gamma^j I^j_t \tag{29}$$

$$R^j_{t+1} = R^j_t + \gamma^j I^j_t, \tag{30}$$

with $\sum_j(S^j_t + I^j_t + R^j_t) \equiv 1$.

As before, atomistic individuals take the average social activity of each group vis-à-vis any other group as given. The first-order condition for the social activity of susceptible individuals belonging to group j vis-à-vis group k now reads as follows:

$$\frac{\partial U(x^{S,j}_{h,t}, x^{S,jk}_{s,t})}{\partial x^{S,jk}_{s,t}} + \beta\eta x^{I,kj}_{s,t}\frac{m^j(\hat{x}^{jk}_{s,t})}{\hat{x}^{jk}_{s,t}}I^k_t(V^{I,j}_{t+1} - V^{S,j}_{t+1}) = 0. \tag{31}$$

The condition is equivalent to that in (24), except that now we have k such first-order conditionss.

Similarly, for infected individuals with altruistic preferences, the first-order condition with respect to social activity of each individual j vis-à-vis any other individual in group k is:

$$\frac{\partial U(x_{h,t}^{I,j}, x_{s,t}^{I,jk})}{\partial x_{s,t}^{I,jk}} + \delta\beta x_{s,t}^{S,kj}\eta\frac{m^k(\hat{x}_{s,t}^{kj})}{\hat{x}_{s,t}^{kj}}I_t^j(V_{t+1}^{I,k} - V_{t+1}^{S,k}) = 0. \tag{32}$$

The first-order conditions for the recovered individuals are the same as in (12), but separately for each group j.

Definition 3. *A decentralized equilibrium for the SIR-network model with a differential choice of group interactions is equivalent to Definition 2, augmented by the k equations* (31) *and* (32) *replacing the previous first-order conditions* (24) *and* (25).

3.6. Social Planner

As noted before, when each person chooses her optimal social activity, she does not consider its impact on the average level of social activity nor on the future course of the number of infected individuals. A social planner takes both into account. The planner's problem is derived for both the homogeneous SIR and the networked SIR with the choice of the average level of social interaction. For the network case we focus on this variant of the model as this already captures the main sources of externality.

The planner is aware of how the average social activity is affected by the density of the matching function (corresponding to, e.g., the geography of the city) and of the future course of infected individuals.[16] The planner knows that in a Nash equilibrium each agent chooses the same amount of social activity, so individual and average social interactions are now the same, hence $x_{s,t}^S = \bar{x}_{s,t}^S$ and $x_{s,t}^I = \bar{x}_{s,t}^I$. This implies that the equilibrium infection rate is given by:

$$p_t^P(.) = \eta x_{s,t}^S x_{s,t}^I (S_t x_{s,t}^S + I_t x_{s,t}^I + R_t x_{s,t}^R)^{(\alpha-1)} I_t. \tag{33}$$

Definition 3: Social Planner in the Homogeneous SIR Model. The social planner

16 The planner is aware of the SIR structure, namely the technological constraints, and can decide on policies taking into account the transitions across the different health states.

chooses the paths of home and social, i.e., outside, activities for each agent by maximizing the weighted sum of the utilities of all agents. The planner is aware of the dependence of the value function of susceptible individuals on the total number of infected and susceptible individuals. Hence, we distinguish between the value function in the decentralized equilibrium and in the planner economy, with the latter denoted as $\hat{V}^i$ where $i = I, S, R$. The planner chooses the sequence $[S_{t+1}, I_{t+1}, R_{t+1}, x^S_{h,t}, x^I_{h,t}, x^R_{h,t}, x^S_{s,t}, x^I_{s,t}, x^R_{s,t}]_{t=0}^{\infty}$ at any initial period t to maximize:

$$\hat{V}^N_t = S_t \hat{V}^S_t(S_t, I_t) + I_t \hat{V}^I_t + R_t \hat{V}^R_t \tag{34}$$

with

$$\hat{V}^S_t(S_t, I_t) = U(x^S_{h,t}, x^S_{s,t}) + \beta[p^P_t(.)V^{\hat{I}}_{t+1} + (1 - p^P_t(.))\hat{V}^S_{t+1}] \tag{35}$$

$$\hat{V}^I_t = U(x^I_{h,t}, x^I_{s,t}) + \delta \hat{V}^S_t(S_t, I_t) + \beta[(1-\gamma)\hat{V}^I_{t+1} + \gamma \hat{V}^S_{t+1}] \tag{36}$$

$$\hat{V}^R_t = U(x^R_{h,t}, x^R_{s,t}) + \beta \hat{V}^R_{t+1} \tag{37}$$

subject to

$$S_{t+1} = S_t - p^P_t(.)S_t \tag{38}$$

$$I_{t+1} = I_t + p^P_t(.)_t S_t - \gamma I_t \tag{39}$$

$$R_{t+1} = R_t + \gamma I_t, \tag{40}$$

where $S_t + I_t + R_t \equiv 1$.

Proposition 1. *The planner reduces social interactions on top and above the decentralized equilibrium. She does so due to a static and a dynamic externality.*

Proof. The first-order conditions for home activities of susceptible and infected individuals and for all activities of the recovered remain the same as in the decentralized equilibrium. The choices of the social activities of susceptible and infected agents are derived in Appendix A. The size of the aggregate inefficiency is obtained from the difference between the first-order conditions for social activities of susceptible and infected individuals in the decentralized

equilibrium, (10) and (18), and the corresponding ones for the social planner's solution, (60) and (61):

$$\chi_t^S = \beta \left[\frac{\partial p_t^P(.)}{\partial x_{s,t}^S} - \frac{p_t}{x_{s,t}^S} \right] [\hat{V}_{t+1}^I - \hat{V}_{t+1}^S] + \beta(1 - p_t^P(.)) \left[\frac{\partial \hat{V}_{t+1}^S}{\partial S_{t+1}} \frac{\partial S_{t+1}}{\partial x_{s,t}^S} + \frac{\partial \hat{V}_{t+1}^S}{\partial I_{t+1}} \frac{\partial I_{t+1}}{\partial x_{s,t}^S} \right] = 0 \quad (41)$$

$$\chi_t^I = \delta \left\{ \beta \left[\frac{\partial p_t^P(.)}{\partial x_{s,t}^I} - \frac{p_t}{x_{s,t}^I} \right] [\hat{V}_{t+1}^I - \hat{V}_{t+1}^S] + \beta(1 - p_t^P(.)) \left[\frac{\partial \hat{V}_{t+1}^S}{\partial S_{t+1}} \frac{\partial S_{t+1}}{\partial x_{s,t}^I} + \frac{\partial \hat{V}_{t+1}^S}{\partial I_{t+1}} \frac{\partial I_{t+1}}{\partial x_{s,t}^I} \right] \right\} = 0, \quad (42)$$

where $p_t^P(.)$ is given by (33).

These differences can be decomposed into two parts corresponding to a static and a dynamic inefficiency.[17] First, atomistic agents do not internalize the impact of their decisions on the average level of social activity, while the planner does. In other words, when choosing their social activity, the atomistic agents take into account the infection rate given by (13), while the social planner takes into account the infection rate given by (33). Hence, the static inefficiency is given by:

$$\Phi_t^S = \beta \left[\frac{\partial p_t^P(.)}{\partial x_{s,t}^S} - \frac{p_t(.)}{x_{s,t}^S} \right] [V_{t+1}^{\hat{I}} - V_{t+1}^{\hat{S}}] \quad (43)$$

$$\Phi_t^I = \delta\beta \left[\frac{\partial p_t^P(.)}{\partial x_{s,t}^I} - \frac{p_t(.)}{x_{s,t}^I} \right] [V_{t+1}^{\hat{I}} - V_{t+1}^{\hat{S}}], \quad (44)$$

where $\frac{p_t(.)}{x_{s,t}^i} = \frac{\partial p_t(.)}{\partial x_{s,t}^i}$, for $i = S, I$. The static inefficiency is affected by the matching function's returns to scale. In places with more dense interactions, the spread of the disease is faster and the size of the inefficiency is larger. This implies that the social planner will adopt stringency or non-pharmaceutical interventions (henceforth NPIs) on top and above the restraints applied by both the susceptible and the infected.

17 These inefficiencies are also considered in Garibaldi et al. (2020) in a different model setup.

The second components that distinguish (60) and (61) from (10) and (18) are:

$$\Psi_t^S = \beta(1 - p_t^P(.)) \left[\frac{\partial \hat{V}_{t+1}^S}{\partial S_{t+1}} \frac{\partial S_{t+1}}{\partial x_{s,t}^S} + \frac{\partial \hat{V}_{t+1}^S}{\partial I_{t+1}} \frac{\partial I_{t+1}}{\partial x_{s,t}^S} \right] \tag{45}$$

$$\Psi_t^I = \delta\beta(1 - p_t^P(.)) \left[\frac{\partial \hat{V}_{t+1}^S}{\partial S_{t+1}} \frac{\partial S_{t+1}}{\partial x_{s,t}^I} + \frac{\partial \hat{V}_{t+1}^S}{\partial I_{t+1}} \frac{\partial I_{t+1}}{\partial x_{s,t}^I} \right]. \tag{46}$$

These terms identify a dynamic inefficiency, which arises since the planner acts under commitment. The planner recognizes that next period's number of infected and susceptible individuals is going to have an effect on the value function of the susceptible individuals through future infection rates.

Definition 4: Social Planner in the SIR-Network Model. In the SIR-network model, the social planner maximizes the sum of future discounted utilities of all groups in the population, taking as given that the infection rates depend on the Nash equilibrium of social interactions. This implies that the infection rates in the networked SIR equilibrium are given by:

$$p_t^{Pj}(.) = x_{s,t}^{S,j} \left[\sum_k \eta \xi_{j,k} x_{s,t}^{I,k} \frac{m^j \left(\sum_k \xi_{j,k} (x_{s,t}^{S,k} S_t^k + x_{s,t}^{I,k} I_t^k + x_{s,t}^{R,k} R_t^k) \right)}{\sum_k \xi_{j,k} (x_{s,t}^{S,k} S_t^k + x_{s,t}^{I,k} I_t^k + x_{s,t}^{R,k} R_t^k)} I_t^k \right]. \tag{47}$$

The planner now chooses the sequence $[S_{t+1}^j, I_{t+1}^j, R_{t+1}^j, x_{h,t}^{S,j}, x_{h,t}^{I,j}, x_{h,t}^{R,j}, x_{s,t}^{S,j}, x_{s,t}^{I,j}, x_{s,t}^{R,j}]_{t=0}^{\infty}$ at any initial period t and for all j to maximize:

$$\hat{V}_t^N = \sum_j [S_t^j \hat{V}_t^{S,j} + I_t^j \hat{V}_t^{I,j} + R_t^j \hat{V}_t^{R,j}] \tag{48}$$

with

$$\hat{V}_t^{S,j}(S_t^j, I_t^j) = U(x_{h,t}^{S,j}, x_{s,t}^{S,j}) + \beta[p_t^{Pj} \hat{V}_{t+1}^{I,j} + (1 - p_t^{Pj}) \hat{V}_{t+1}^{S,j}] \tag{49}$$

$$\hat{V}_t^{I,j} = U(x_{h,t}^{I,j}, x_{s,t}^{I,j}) + \delta \sum_j \hat{V}_t^{S,j}(S_t^j, I_t^j) + \beta[(1 - \gamma) \hat{V}_{t+1}^{I,j} + \gamma \hat{V}_{t+1}^{S,j}] \tag{50}$$

$$\hat{V}_t^{R,j} = U(x_{h,t}^{R,j}, x_{s,t}^{R,j}) + \beta[\hat{V}_{t+1}^{R,j}] \tag{51}$$

subject to

$$S_{t+1}^j = S_t^j - p_t^{Pj}(.)S_t^j \tag{52}$$

$$I_{t+1}^j = I_t^j + p_t^{Pj}(.)S_t^j - \gamma I_t^j \tag{53}$$

$$R_{t+1}^j = R_t^j + \gamma I_t^j, \tag{54}$$

where $\sum_j (S_t^j + I_t^j + R_t^j) \equiv 1$. The full set of first-order conditions can be found in Appendix B.

Proposition 2. *The inefficiencies in the SIR-network model are larger than in the homogeneous SIR model, and also take into account the reciprocal relations.*

Proof. The first-order conditions of the planner problem can be found in Appendix B. Comparing those, i.e., (62) and (63), with the corresponding ones from the decentralized equilibrium of the SIR-network model, we obtain the following aggregate inefficiencies for each group j:

$$\Omega_t^{S,j} = \beta \left[\frac{\partial p_t^{Pj}(.)}{\partial x_{s,t}^{S,j}} - \frac{\partial p_t^j}{\partial x_{s,t}^{S,j}} \right] [\hat{V}_{t+1}^{I,j} - \hat{V}_{t+1}^{S,j}] + \beta(1 - p_t^{Pj}(.)) \sum_k \left[\frac{\partial \hat{V}_{t+1}^{S,j}}{\partial S_{t+1}^k} \frac{\partial S_{t+1}^k}{\partial x_{s,t}^{S,j}} + \frac{\partial \hat{V}_{t+1}^{S,j}}{\partial I_{t+1}^k} \frac{\partial I_{t+1}^k}{\partial x_{s,t}^{S,j}} \right] = 0 \tag{55}$$

$$\Omega_t^{I,j} = \delta\beta \sum_k \left\{ \left[\frac{\partial p_t^{Pk}(.)}{\partial x_{s,t}^{I,j}} - \frac{\partial p_t^k}{\partial x_{s,t}^{I,j}} \right] [\hat{V}_{t+1}^{I,k} - \hat{V}_{t+1}^{S,k}] + (1 - p_t^{Pk}(.)) \sum_n \left[\frac{\partial \hat{V}_{t+1}^{S,k}}{\partial S_{t+1}^n} \frac{\partial S_{t+1}^n}{\partial x_{s,t}^{I,j}} + \frac{\partial \hat{V}_{t+1}^{S,k}}{\partial I_{t+1}^n} \frac{\partial I_{t+1}^n}{\partial x_{s,t}^{I,j}} \right] \right\} = 0. \tag{56}$$

For the SIR-network model, the inefficiencies contain additional components. First of all, the static inefficiency is summed across all groups j. Second, the dynamic inefficiency is weighted by a probability that takes into account the summation of the infection rates across groups. These additional terms capture a reciprocity externality. The planner is aware that the social activity has a differential impact across age groups, which is reflected in the size of the externality.

Having characterized the inefficiencies, we turn to discussing actual implementation policies in the homogeneous SIR and the SIR-network model, and their suitability to close the inefficiencies.

3.7. Implementability: Partial Lockdown in the Homogeneous SIR Model and Targeted Lockdown in the SIR-Network Model

In this section, we examine which lockdown policies are efficient. In particular, we consider partial and targeted lockdown policies.

Partial Lockdown in SIR. A partial lockdown can be examined also in the simple homogeneous SIR model. θ is defined as the fraction of social activity that is restricted. The planner can enforce two different lockdown policies, θ^S and θ^I, only if there is the possibility to identify infected individuals. Let us first assume they cannot be identified, so the social activity of all agents will be restricted.[18] Furthermore, there is only a unique θ. Then, a partial lockdown policy affects the infection probability in the decentralized economy as follows:

$$p_t(\theta, .) = \eta(1-\theta)x^S_{s,t}(1-\theta)x^I_{s,t}\frac{m((1-\theta)\bar{x}_{s,t})}{(1-\theta)\bar{x}_{s,t}}I_t. \tag{57}$$

Lemma 2. *The partial lockdown policy is efficient only in the presence of the means to identify infected individuals, such as universal testing.*

Proof. The partial lockdown policy would be efficient if it set the aggregate inefficiencies equal to zero, that is:

$$\beta\left[\frac{\partial p^P_t(.)}{\partial x^S_{s,t}} - \frac{p_t}{x^S_{s,t}}\right][\hat{V}^I_{t+1} - \hat{V}^S_{t+1}] + \beta(1-p^P_t(.))\left[\frac{\partial \hat{V}^S_{t+1}}{\partial S_{t+1}}\frac{\partial S_{t+1}}{\partial x^S_{s,t}} + \frac{\partial \hat{V}^S_{t+1}}{\partial I_{t+1}}\frac{\partial I_{t+1}}{\partial x^S_{s,t}}\right] = 0 \tag{58}$$

$$\delta\beta\left\{\left[\frac{\partial p^P_t(.)}{\partial x^I_{s,t}} - \frac{p_t}{x^I_{s,t}}\right][\hat{V}^I_{t+1} - \hat{V}^S_{t+1}] + (1-p^P_t(.))\left[\frac{\partial \hat{V}^S_{t+1}}{\partial S_{t+1}}\frac{\partial S_{t+1}}{\partial x^I_{s,t}} + \frac{\partial \hat{V}^S_{t+1}}{\partial I_{t+1}}\frac{\partial I_{t+1}}{\partial x^I_{s,t}}]\right]\right\} = 0. \tag{59}$$

Equations (58) and (59) include both the static and the dynamic inefficiency. If the planner is endowed with a single instrument, i.e., a single lockdown policy applied equally to both susceptible and infected individuals, she cannot close these two inefficiencies at once. Only in

18 Some individuals might not have any symptoms and are not tested.

the presence of a second instrument, specifically a measure to identify infected individuals, she can target policies toward agents in these two states and set the inefficiencies to zero.

Targeted Lockdown Policies in the SIR-Network Model. In the SIR-network model, the planner could consider targeted policies, i.e., different degrees of stringency measures targeted at different groups.

Lemma 3. *Implementable targeted lockdown policies require differentiated fractions θ_j^S and θ_j^I for susceptible and infected individuals of each group. This can be achieved only with the additional instrument of testing.*

Proof. Targeted lockdown policies would be efficient if they could set to zero the aggregate inefficiencies stemming from (55) and (56). This would imply different θ_j^S and θ_j^I that can close the $2j$ inefficiencies. This can be achieved only by means of identifying and isolating infected from susceptible individuals.

4. Simulations

In this section, we simulate different variants of our model, for both the decentralized equilibrium and the social planner's equilibrium. The primary goal is to ascertain the impact of social-activity choices on the dynamics of infections by comparing our baseline optimizing SIR model to the traditional version with exogenous contact rates. Furthermore, by comparing the simulations of the homogeneous SIR model with and without altruism, we assess the latter's importance. Finally, simulations of the SIR-network model highlight the role of reciprocity and homophily.

Overall, all model variants in which agents adjust their social activity in response to risk, altruism, and homophily exhibit a flattened infection curve compared to the traditional SIR model. This enhances the salience of our model implications. Policymakers designing mitigation policies shall be aware of the agents' responses to risk, also conditional on their social, cultural, and community traits.

4.1. Comparison Homogeneous SIR Model with Optimizing Individuals and Standard SIR Model

The model is solved numerically through a classical Newton-Raphson algorithm that computes the transition from one steady state to the next, with the latter induced by an infection shock leading to changes in the number of infected individuals in the population. The model calibration is as follows. The instantaneous utility of the susceptible and infected is a function of their social activities $x^S_{s,t}$ and $x^I_{s,t}$, respectively.[19] The functional forms read as follows: $U(x^S_{s,t}) = x^S_{s,t} - \frac{(x^S_{s,t})^2}{2c_S}$ and $U(x^I_{s,t}) = x^I_{s,t} - \frac{(x^I_{s,t})^2}{2c_I} - C_I$, where C_I is the cost of being sick, and we set $c_S = 1$ and $c_I = 0.3$. The latter implies that some infected individuals might not feel well and, therefore, on average have a lower level of social activity. In general, C_I might depend on the congestion of the health system, which in turn depends on the number of infected individuals. We abstract from this dependence, but note that its inclusion would actually strengthen our conclusions: infected individuals aware of the health-system congestion would reduce their social activity even more.

The cost of being sick is set equal to 10. This is a relatively high value, which reflects fear of severe long-term health complications or even death. Recall that for simplicity, in our analytical derivations we have assumed a death rate of zero, so it is reasonable to include its impact among the costs of the infection. Following Newman (2018), we set the recovery rate γ to 0.4. Furthermore, β is set to 0.96, α to 1, and δ to 0.5. Following Garibaldi et al. (2020), we set $\eta = 2.4$, which combines a constant term from the matching function and the exogenous transmission rate of COVID-19.

Figure 1 below compares the dynamics of the numbers of infected, susceptible, and recovered individuals both in our homogeneous SIR model with endogenous social activity and in the traditional SIR model with exogenous contact rates. For the sake of comparison, in the latter the social activity is set to a constant value equal to the average steady-state social activity, i.e., 0.65. The other parameters are the same across the two models. Furthermore,

19 We assume that in steady state the utility functions of recovered and susceptible individuals are the same. Recovered individuals do not modify their social activity since they become immune. This is realistic at least for a certain length of time. Furthermore, in the simulations we do not analyze the home activities since they do not matter for our results.

Figure 2 shows the dynamics of social activity chosen by susceptible and infected individuals relative to the steady state levels and compares the models with and without altruism.

First and foremost, Figure 1 shows that the peak of the infection curve (middle panel) is significantly flattened in the model with endogenous social activity. The number of susceptible individuals remains higher in the optimizing SIR model. As the disease takes its course, the number of infected individuals increases more sluggishly over time. An exact quantification of this effect could be useful for the planning of health care units. Second, Figure 2 shows that the social interaction of infected individuals (left panel) is unchanged over time in the absence of altruism, while it decreases significantly in the presence of altruism. Interestingly, in the presence of altruism, susceptible individuals decrease their social contacts by less, since a large part of the burden is carried by the infected individuals.

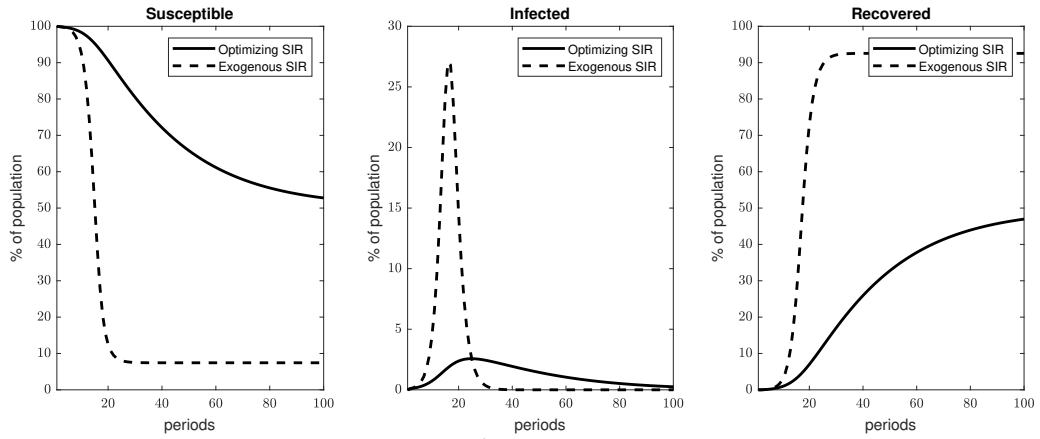

Figure 1
Comparison of the Homogeneous SIR Model with Endogenous Social Activity and the Traditional SIR Model with Constant Exogenous Contact Rates

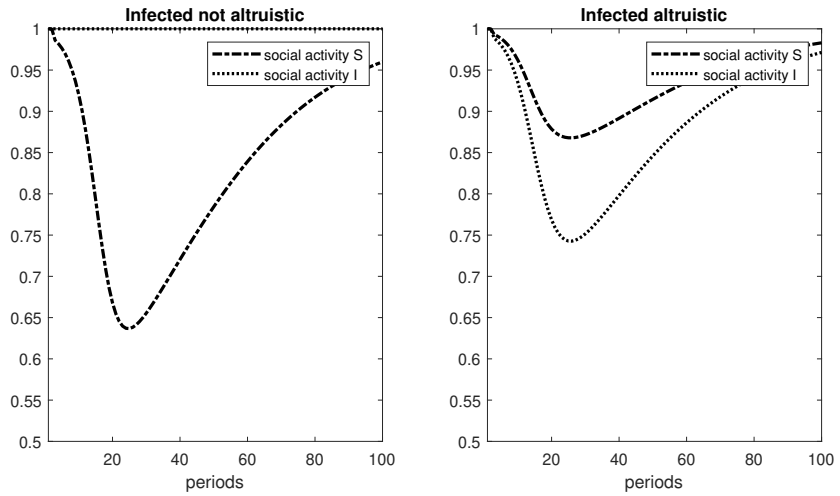

Figure 2
Comparison of Social Activity of Infected and Susceptible Individuals in the Homogeneous SIR Model with (right panel) and without Altruism (left panel)

4.1.1. Comparison SIR-Network Model with Endogenous Social Activity and Standard SIR-Network Model

In the SIR-network model, three age groups are included.[20] Following Acemoglu et al. (2020), the three groups are the young ($20-49$ years), middle-aged ($50-64$ years), and old (65+ years). The respective population shares are set to $N_y = 53\%$, $N_m = 26\%$, and $N_o = 21\%$. The network adjacency or homophily matrix is calibrated so that all groups have a contact rate, $\xi_{j,k}$, equal to 1 with their peers and equal to 0.7 (or later on 0.4) with the other groups. The matrix is symmetric, reflecting reciprocal contact rates between groups. This calibration is similar to that in Acemoglu et al. (2020), which facilitates the comparison of our SIR-network model with endogenous social activity and other SIR-network models with exogenous contact rates and similar age structures. Realistically, different age groups have different recovery rates. For the middle-aged group, we set $\gamma_m = 0.4$, a number that is standard in the literature; for the younger group, a slightly faster recovery $\gamma_y = 0.45$ is chosen, and for the older group, we set $\gamma_o = 0.35$. All other parameters are kept as in the benchmark homogeneous SIR model.

Figure 3 compares the dynamics of infected, susceptible, and recovered individuals in our SIR-network model (thicker lines) with those in the exogenous SIR-network model (thinner

20 An extension to more groups is feasible, but would not change the main implications.

lines).[21] The latter case is obtained by setting the social activity of each group equal to their respective steady-state values. The comparison is again revealing. In our SIR-network model, the curves for the infected of all age groups are much flatter than those in the exogenous SIR-network model. Figure 4 displays the social activity of susceptible individuals of all three age groups for our model. While young, middle-aged, and old agents all reduce their social activities, the old group reduces it by more since its agents are more exposed to the severe health risk and the corresponding utility loss due to their lower recovery rate.

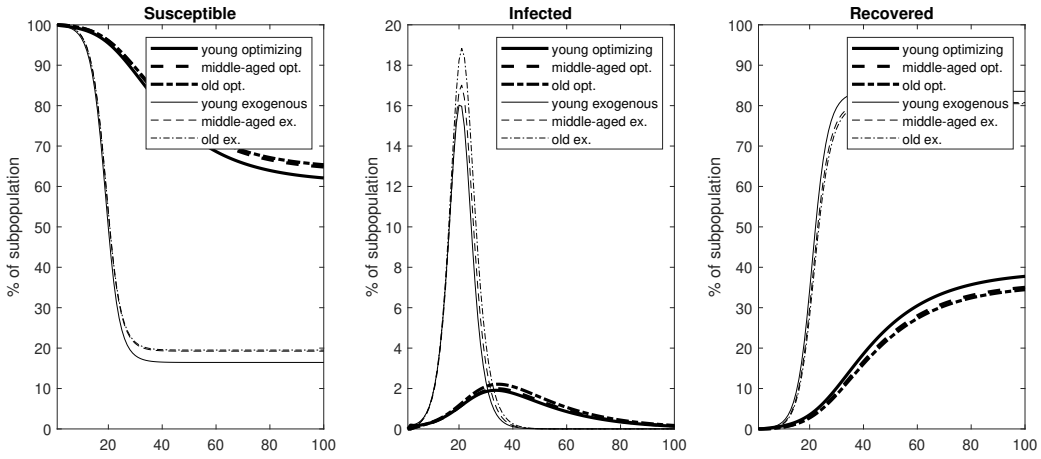

Figure 3
Comparison of SIR-Network Models with Endogenous Social Activity vs. Constant Exogenous Contact Rates

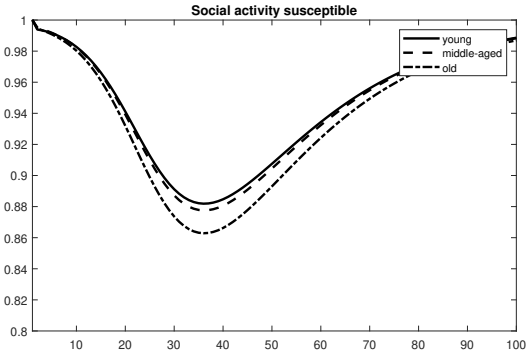

Figure 4
Dynamics of Social Interactions of Age Groups in the SIR-Network Model with Endogenous Social Activity

21 The initial infection shock is set to 0.001 and takes place in the young group, i.e., the group with a presumably higher social-activity intensity.

4.1.2. SIR-Network Model with Endogenous Choice of Group-Differentiated Social Activity

Thus far, we have kept the reciprocal degree of contact across groups, ξ_{jk}, fixed and allowed for an endogenous decision of the general intensity of social interactions. The rationale for this is that interactions vis-à-vis specific groups are partly the result of organizational and societal practices, culture, and attitudes, which prevail above and beyond agents' decisions on a daily basis. We are, however, interested in assessing the performance of our model along several possible dimensions, including the case in which agents endogenously choose even the degree of social interactions for each specific group. In Section (3.5), we have shown how the analytics of the model would change in this case: an important insight from equation 31 is that an agent choosing social intensity with group k internalizes only the infection risk toward this group, as opposed to the sum (as per equation (24)). This changes the incentives as our simulations will further clarify.

To isolate the specific effects of the endogenous differential contacts, the steady state is calibrated so as to make the new model variant comparable to the previous one.[22] The levels of the infection probabilities are lower in the new model (see Figure 9 in Appendix C). As agents now decide on differential contacts, they can also avoid the most dangerous group, the young ones in our case, that interacts the most. The young ones can also differentiate and, more specifically, avoid contact with the most fragile group.

While the levels of the infection probabilities are lower, their changes are larger. This is so, since, as highlighted in the analytical part, individuals choosing group-based social intensity now internalize the risk vis-à-vis specific groups as opposed to the aggregate. In other words, in this new variant of the model, individuals only consider direct exposure to each group separately and neglect the indirect exposure through the rows of the network matrix, as before.[23]

22 Specifically, $x_{s,t}^{S,jj} = 1$ and $x_{s,t}^{S,jk} = 0.7$ in the steady state. As before, the steady-state levels of social activity for infected individuals are multiplied by 0.3 to take into account that the symptomatic ones can isolate themselves.

23 As this form of neglect might not be completely realistic, we adjust the cost of infections to $C_I = 20$. This is economically equivalent to having individuals internalize infection costs, such as hospital congestion.

Beyond the aggregate dynamic, it is of interest also to examine the activity of each group. Figure 5 shows the social-activity intensities of young, middle-aged, and old susceptible agents vis-à-vis the three different groups relative to their steady-state levels. First, all three groups reduce their contacts to the young the most, as those are the most significant spreaders.[24] Second, each group reduces significantly the contacts with their peers: social interactions along the diagonal of the adjacency matrix are the most intense to start with, hence they are more conducive to risk. Figure 6 shows the aggregate level of social-activity intensity of all three susceptible age groups relative to the steady state. The aggregate dynamic is strikingly similar to the one in Figure 4, which depicts the previous model variant. However, we have seen that the aggregate may mask individual group dynamics which can differ significantly between the two models.

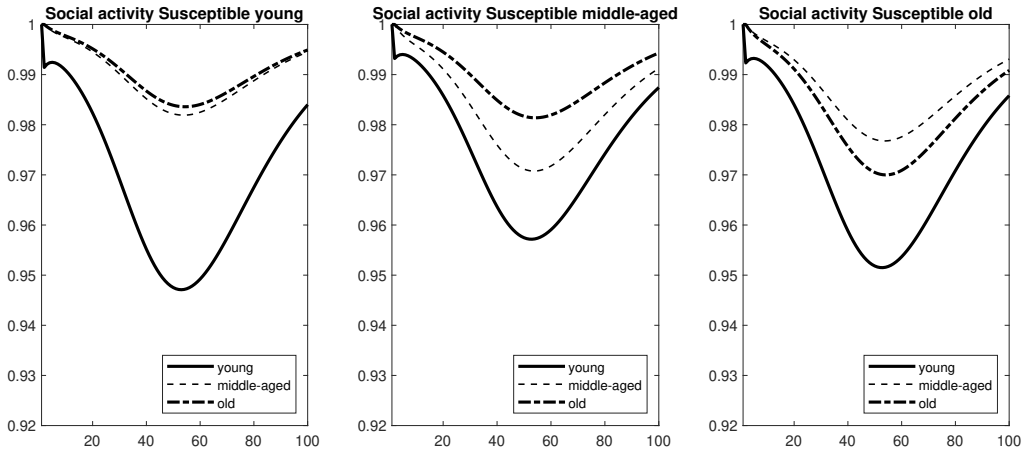

Figure 5
Differentiated Social Activities relative to Steady-State Levels in the SIR-Network Model with Endogenous Group-Differentiated Social Activity

24 Figure 10 in Appendix C displays the pandemic's dynamic. The young ones are in the group with the highest share of infected agents.

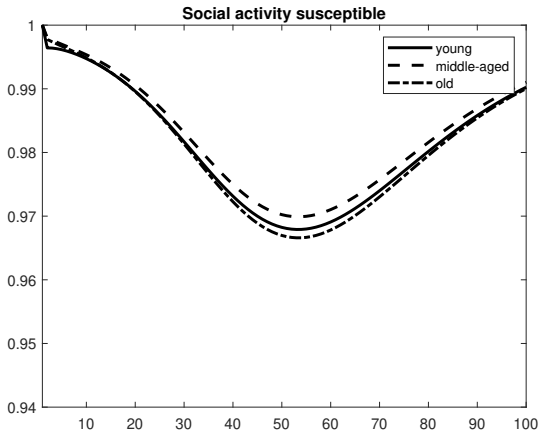

Figure 6
Aggregate Social Activities relative to Steady-State Levels in the SIR-Network Model with Endogenous Group-Differentiated Social Activity

4.2. Optimal Lockdown Policy in the Homogeneous SIR and the SIR-Network Model: Social Planner's Solution

We now quantify the optimal lockdown policy and its dependence on the preference and community structure, for both the homogeneous SIR and the networked SIR model.[25] Figure 7 plots the optimal lockdown policy as captured by the fraction θ chosen by the planner (right panel) and the resulting social interactions of the susceptible individuals in our homogeneous SIR model with optimizing agents. The parameters are as before with δ set to 0.5 and 0 for the model variants with and without altruism, respectively. Each panel of Figure 7 compares the cases with (dashed line) and without (solid line) altruism. Interestingly, and in accordance with our empirical results, the planner chooses a smaller fraction of locked-down activities when individuals are altruistic. Again, social interactions of susceptible individuals are higher in the altruistic case. This is because infected individuals adjust their interactions already by themselves in consideration of other people's infection risk.

Figure 8 plots the optimal lockdown policy (right panel) and the resulting social interactions of susceptible agents (left panel) for the planner's solution in the SIR-network model. Here, lockdown policies are set differentially across age groups. While a full lockdown of a single group (sequestering) jointly with full freedom for the others would be unethical, joint burden

25 Since qualitatively the responses of social activities are similar, we use the SIR-network model with fixed degrees of homophily in this section.

sharing with differential protective NPIs across groups is desirable in light of the different recovery rates.[26] A practical implementation of this policy would include more extensive leave of absence for workers in older age groups or in groups with pre-existing health conditions.

Our results point to two main conclusions. First, stringency measures are stricter for the greatest risk spreaders, namely the age group in which the infection shock happened and which has a higher social-activity intensity. Second, each panel compares the cases where individuals hold different degrees of homophily, by setting $\xi = 0.7$ (lower homophily, black lines) and $\xi = 0.4$ (higher homophily, blue lines). Interestingly, stringency measures are generally stricter in the case of lower homophily. Lower homophily implies that an infection outbreak, occurring within one group, spreads faster to the other groups. Hence, in order to curb the epidemic, the planner optimally shall restrict social activity in the affected group by more.

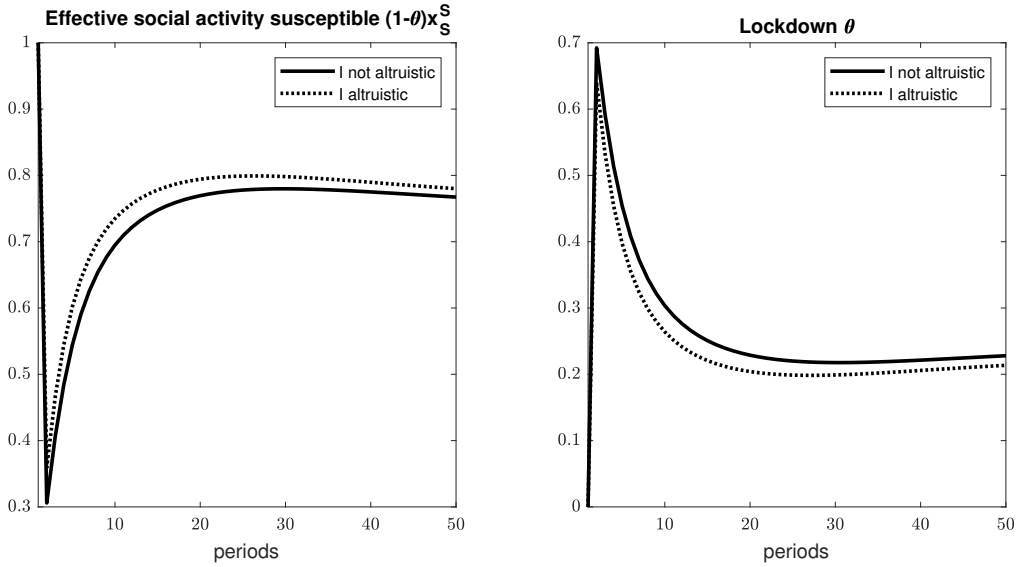

Figure 7
Social Activity of Susceptible Individuals and Optimal Lockdown Depending on Degree of Altruism of Infected Individuals

26 Recall that different recovery rates also implicitly capture different mortality rates.

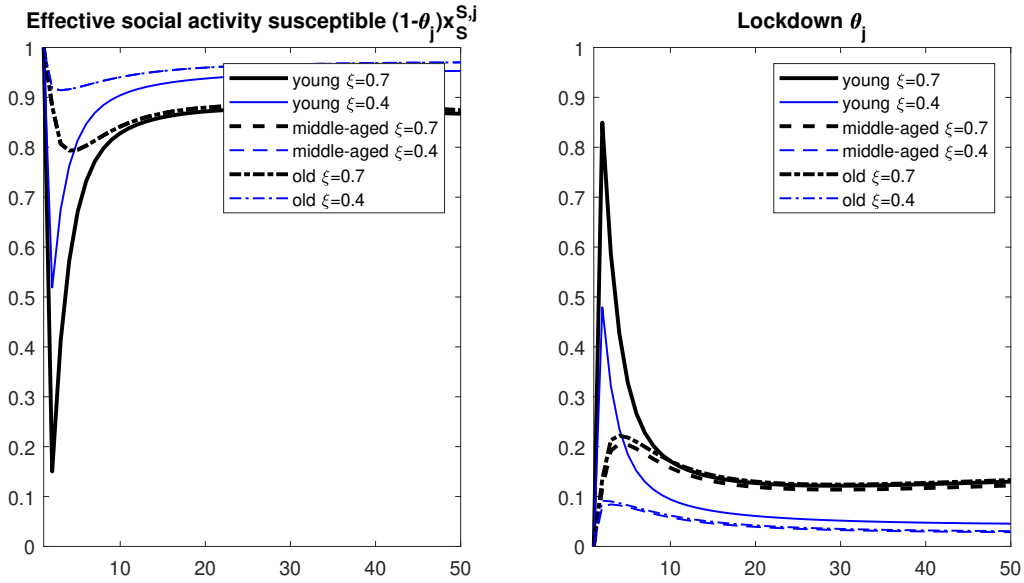

Figure 8
Social Activity of Susceptible Individuals and Optimal Differentiated Lockdown Policies for Different Degrees of Group Connections

5. Concluding Remarks

While envisaging a return to freedom of mobility and to past customs, though hopefully with fading fears, understanding the determinants of people's behavior in the face of catastrophic events is important along at least two dimensions. First, it is difficult to accurately forecast the spread of a disease with models that do not account for human behavior. Second, as policymakers seek advice on exit strategies that could mitigate both the loss of lives and the economic consequences, understanding individuals' behavior, even as lockdowns or other stringency measures are lifted, is informative. Excessive precautionary behavior is likely to trigger demand spirals which might slow down the recovery process.

One of the initial approaches to contain the pandemic, suggested by experts, has been a "one size fits all" response, namely a full lockdown. We uncover important heterogeneities in individuals' behavior as well as in the efficacy of stringency measures with respect to regional differences in time and space. Our findings suggest that a balanced approach involving a joint interaction of stringency measures, in respect of human dignity, and responsible social preferences can help mitigate both the public health crisis and the economic costs. A

social planner does wish to impose stringency measures, due to various externalities, but they depend on the social, cultural, and community traits. Stringency measures are stricter for agents with high social intensity and when groups exhibit less homophily, i.e., when the disease is less likely to be confined to one group, and can spread more easily within communities.

References

Acemoglu, D., Chernozhukov, V., Werning, I., and Whinston, M. D. (2020). Optimal Targeted Lockdowns in a Multi-Group SIR Model. *NBER Working Paper No. 27102*.

Alfaro, L., Faia, E., Lamersdorf, N., and Saidi, F. (2020). Social Interactions in Pandemics: Fear, Altruism, and Reciprocity. *NBER Working Paper No. 27134*.

Ambrus, A., Mobius, M., and Szeidl, A. (2014). Consumption Risk-Sharing in Social Networks. *American Economic Review*, 104(1):149–182.

Andreoni, J. (1989). Giving with Impure Altruism: Applications to Charity and Ricardian Equivalence. *Journal of Political Economy*, 97(6):1447–1458.

Andreoni, J. (1993). An Experimental Test of the Public-Goods Crowding-Out Hypothesis. *American Economic Review*, 83(5):1317–1327.

Andreoni, J. and Miller, J. (2002). Giving according to GARP: An Experimental Test of the Consistency of Preferences for Altruism. *Econometrica*, 70(2):737–753.

Bailey, M., Cao, R., Kuchler, T., and Stroebel, J. (2018). The Economic Effects of Social Networks: Evidence from the Housing Market. *Journal of Political Economy*, 126(6):2224–2276.

Bailey, M., Johnston, D., Koenen, M., Kuchler, T., Russel, D., and Stroebel, J. (2020). Social Distancing during a Pandemic: The Role of Friends. *NBER Working Paper No. 28234*.

Becker, G. (1974). A Theory of Social Interactions. *Journal of Political Economy*, 82(6):1063–1093.

Becker, G. S. (1996). Preferences and Values. In *Accounting for Tastes*, pages 1–23. Harvard University Press.

Berg, J., Dickhaut, J., and McCabe, K. (1995). Trust, Reciprocity, and Social History. *Games and Economic Behavior*, 10(1):122–142.

Bloch, F., Génicot, G., and Ray, D. (2008). Informal Insurance in Social Networks. *Journal of Economic Theory*, 143(1):36–58.

Bohnet, I. and Frey, B. S. (1999). Social Distance and Other-Regarding Behavior in Dictator Games: Comment. *American Economic Review*, 89(1):335–339.

Bolton, G. E. and Ockenfels, A. (2000). ERC: A Theory of Equity, Reciprocity, and Competition. *American Economic Review*, 90(1):166–193.

Bramoullé, Y. and Kranton, R. (2007). Risk-Sharing Networks. *Journal of Economic Behavior & Organization*, 64(3-4):275–294.

Brock, W. A. and Durlauf, S. N. (2001). Discrete Choice with Social Interactions. *Review of Economic Studies*, 68(2):235–260.

Case, A. C. and Katz, L. F. (1991). The Company You Keep: The Effects of Family and Neighborhood on Disadvantaged Youths. Technical report.

Cicala, S., Fryer, R. G., and Spenkuch, J. L. (2018). Self-Selection and Comparative Advantage in Social Interactions. *Journal of the European Economic Association*, 16(4):983–1020.

Currarini, S., Jackson, M. O., and Pin, P. (2009). An Economic Model of Friendship: Homophily, Minorities, and Segregation. *Econometrica*, 77(4):1003–1045.

Diamond, P. A. (1982). Aggregate Demand Management in Search Equilibrium. *Journal of Political Economy*, 90(5):881–894.

Falk, A., Becker, A., Dohmen, T., Enke, B., Huffman, D., and Sunde, U. (2018). Global Evidence on Economic Preferences. *Quarterly Journal of Economics*, 133(4):1645–1692.

Farboodi, M., Jarosch, G., and Shimer, R. (2020). Internal and External Effects of Social Distancing in a Pandemic. *NBER Working Paper No. 27059*.

Fehr, E. and Gächter, S. (2000). Fairness and Retaliation: The Economics of Reciprocity. *Journal of Economic Perspectives*, 14(3):159–181.

Fehr, E. and Schmidt, K. M. (1999). A Theory of Fairness, Competition, and Cooperation. *Quarterly Journal of Economics*, 114(3):817–868.

Garibaldi, P., Moen, E. R., and Pissarides, C. A. (2020). Modelling Contacts and Transitions in the SIR Epidemics Model. *Covid Economics: Vetted and Real-Time Papers*, 5.

Glaeser, E. L., Sacerdote, B., and Scheinkman, J. A. (1996). Crime and Social Interactions. *Quarterly Journal of Economics*, 111(2):507–548.

Hethcote, H. W. (2000). The Mathematics of Infectious Diseases. *SIAM Review*, 42(4):599–653.

Hofstede, G. (2001). *Culture's Consequences: Comparing Values, Behaviors, Institutions and Organizations across Nations*. Sage Publications.

Kermack, W. O. and McKendrick, A. G. (1927). A Contribution to the Mathematical Theory of Epidemics. *Proceedings of the Royal Society of London*, 115(772):700–721.

Moinet, A., Pastor-Satorras, R., and Barrat, A. (2018). Effect of Risk Perception on Epidemic Spreading in Temporal Networks. *Physical Review E*, 97:012313.

Moser, C. A. and Yared, P. (2020). Pandemic Lockdown: The Role of Government Commitment. *NBER Working Paper No. 27062*.

Newman, N. (2018). *Networks.* Oxford University Press, 2nd edition.

Pastor-Satorras, R. and Vespignani, A. (2001a). Epidemic Dynamics and Endemic States in Complex Networks. *Physical Review E*, 63(6):066117.

Pastor-Satorras, R. and Vespignani, A. (2001b). Epidemic Spreading in Scale-Free Networks. *Physical Review Letters*, 86(14):3200–3203.

Perra, N., Gonçalves, B., Pastor-Satorras, R., and Vespignani, A. (2012). Activity Driven Modeling of Time Varying Networks. *Scientific Reports*, 2(469).

Petrongolo, B. and Pissarides, C. A. (2001). Looking into the Black Box: A Survey of the Matching Function. *Journal of Economic Literature*, 39(2):390–431.

Pissarides, C. A. (2000). *Equilibrium Unemployment Theory*. The MIT Press, 2nd edition.

Spolaore, E. and Wacziarg, R. (2013). How Deep are the Roots of Economic Development? *Journal of Economic Literature*, 51(2):325–369.

Wu, L. and Shimer, R. (2021). Endogenous Homophily. Mimeo.

A. First-Order Conditions of the Social Planner in the Homogeneous SIR Model

The first-order conditions for the social planner's problem in Definition 3 for the home activity of infected and susceptible individuals and for the home and outside activities of recovered individuals are equivalent to the ones obtained under the decentralized equilibrium. For the social activity of susceptible and infected individuals, however, we have:

$$\frac{\partial U(x_{h,t}^S, x_{s,t}^S)}{\partial x_{s,t}^S} + \beta \frac{\partial p_t^P(.)(.)}{\partial x_{s,t}^S}[(\hat{V}_{t+1}^I - \hat{V}_{t+1}^S] + \beta(1 - p_t^P(.)) \left[\frac{\partial \hat{V}_{t+1}^S}{\partial S_{t+1}} \frac{\partial S_{t+1}}{\partial x_{s,t}^S} + \frac{\partial \hat{V}_{t+1}^S}{\partial I_{t+1}} \frac{\partial I_{t+1}}{\partial x_{s,t}^S} \right] = 0 \quad (60)$$

$$\frac{\partial U(x_{h,t}^I, x_{s,t}^I)}{\partial x_{s,t}^I} + \delta \left\{ \beta \frac{\partial p_t^P(.)}{\partial x_{s,t}^I}[(\hat{V}_{t+1}^I - \hat{V}_{t+1}^S] + \beta(1 - p_t^P(.)) \left[\frac{\partial \hat{V}_{t+1}^S}{\partial S_{t+1}} \frac{\partial S_{t+1}}{\partial x_{s,t}^I} + \frac{\partial \hat{V}_{t+1}^S}{\partial I_{t+1}} \frac{\partial I_{t+1}}{\partial x_{s,t}^I} \right] \right\} = 0. \quad (61)$$

B. First-Order Conditions of the Social Planner in the SIR-Network Model

The first-order conditions for the social planner's problem in Definition 4 for the home activity of infected and susceptible individuals and for the home and outside activities of recovered individuals are equivalent to the ones obtained under the decentralized equilibrium. For the social activity of susceptible and infected individuals in each group j, however, the first-order conditions are as follows:

$$\frac{\partial U(x_{h,t}^{S,j}, x_{s,t}^{S,j})}{\partial x_{s,t}^{S,j}} + \beta \frac{\partial p^{Pj}(.)}{\partial x_{s,t}^{S,j}}[\hat{V}_{t+1}^{I,j} - \hat{V}_{t+1}^{S,j}] + \beta(1 - p_t^{Pj}(.)) \sum_k \left[\frac{\partial \hat{V}_{t+1}^{S,j}}{\partial S_{t+1}^k} \frac{\partial S_{t+1}^k}{\partial x_{s,t}^{S,j}} + \frac{\partial \hat{V}_{t+1}^{S,j}}{\partial I_{t+1}^k} \frac{\partial I_{t+1}^k}{\partial x_{s,t}^{S,j}} \right] = 0 \quad (62)$$

$$\frac{\partial U(x_{h,t}^{I,j}, x_{s,t}^{I,j})}{\partial x_{s,t}^{I,j}} + \delta\beta \sum_k \left\{ \frac{\partial p^{Pk}(.)}{\partial x_{s,t}^{I,j}} [(\hat{V}_{t+1}^{I,k} - \hat{V}_{t+1}^{S,k}] + (1 - p_t^{Pk}(.)) \sum_n \left[\frac{\partial \hat{V}_{t+1}^{S,k}}{\partial S_{t+1}^n} \frac{\partial S_{t+1}^n}{\partial x_{s,t}^{I,j}} + \frac{\partial \hat{V}_{t+1}^{S,k}}{\partial I_{t+1}^n} \frac{\partial I_{t+1}^n}{\partial x_{s,t}^{I,j}} \right] \right\} = 0. \tag{63}$$

C. Additional Figures

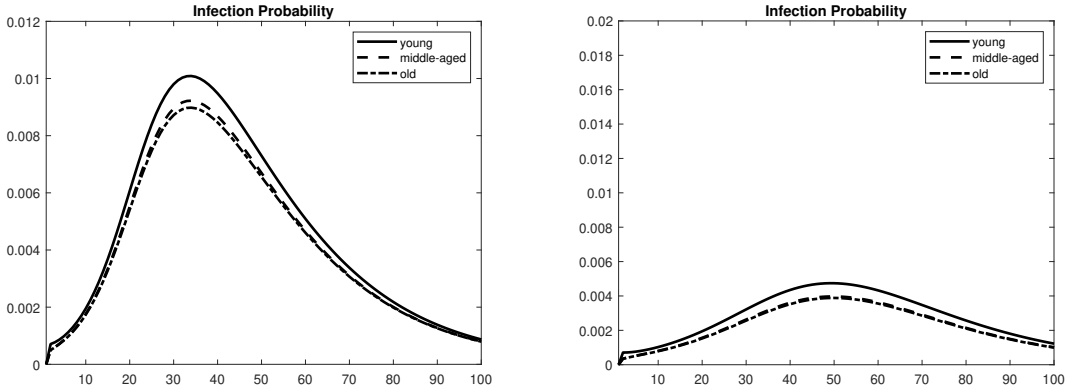

(a) Baseline SIR-Network Model (b) Group-differentiated Social Activity

Figure 9
Dynamics of Infection Probabilities in the SIR-Network Model

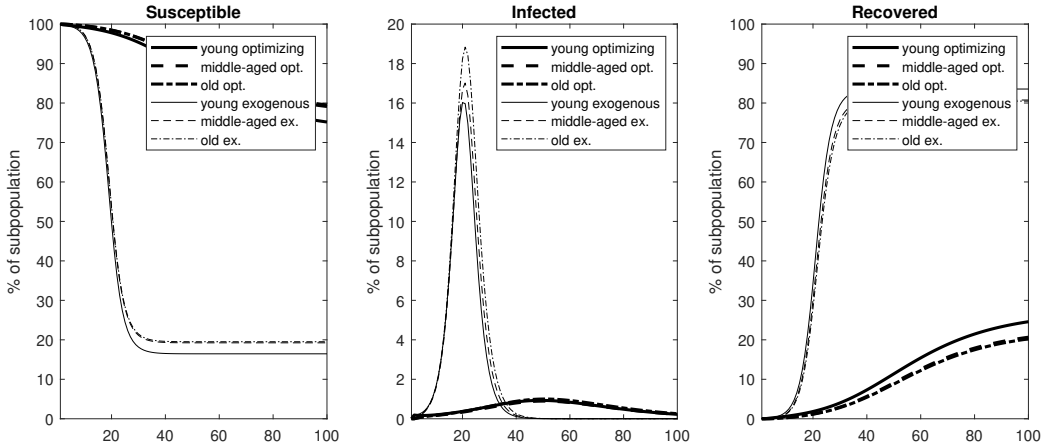

Figure 10
Comparison of SIR-Network Models with Endogenous Group-differentiated Social Activity vs. Constant Exogenous Contact Rates